Chemical Physics Letters 530 (2012) 39–44

Contents lists available at SciVerse ScienceDirect

Chemical Physics Letters

journal homepage: www.elsevier.com/locate/cplett

Theoretical study of conjugated polyelectrolyte electron injection layers: Effects of counterions, charged groups and charge reversal

Huyen Thi Nguyen [a], Thuc-Quyen Nguyen [b], Minh Tho Nguyen [a,c,*]

[a] Department of Chemistry, University of Leuven, B-3001 Leuven, Belgium
[b] Department of Chemistry and Biochemistry, Center for Polymers and Organic Solids, University of California, Santa Barbara, CA 93106, USA
[c] Institute for Computational Science and Technology (ICST), HoChiMinh City, Viet Nam

ARTICLE INFO

Article history:
Received 26 November 2011
In final form 31 January 2012
Available online 7 February 2012

ABSTRACT

The molecular structures, electronic and charge-transport properties of three conjugated polyelectrolytes (CPEs) including $PFPhCO_2Na$, $PFPhSO_3Na$, and $PFPhBIm_4$ are studied using the density functional theory with B3LYP functional. The charge injection and charge transport properties are investigated through the ionization energies, electron affinities, lowest allowed excitation energies, reorganization energies and electron transfer integrals. The electron/hole injections have great effect on the planarity of cationic/anionic CPEs. The band gaps of the CPEs do not vary significantly with the charged groups and counterions. Charge-transport properties show that the $PFPhSO_3Na$ and $PFPhBIm_4$ are good candidates for electron-transport materials.

1. Introduction

Conjugated polyelectrolytes (CPEs) form a class of organic semiconducting materials having a π-conjugated backbone with pendant ionic groups. The latter are ionized in high dielectric media, thereby rendering the CPE materials soluble in water and other polar solvents [1]. Being exploited since the mid 1980s [2,3], the CPEs have very unique characteristics which include a combination of the optical and electronic properties of both conjugated polymers [4] and polyelectrolytes. Properties of the latter are modulated by complexes containing long range electrostatic interactions [5,6]. The solubility and large optical cross sections of CPEs led to their extensive applications in biosensors where the conjugated backbone plays the light-harvesting role [7,8]. CPEs with the presence of charged counterions also function as single component active layers in light-emitting electrochemical cells (LECs) [9,10]. Recently, there has been an upsurge in using CPEs as electron transport/injection layers (ETLs) in polymer light emitting diodes (PLEDs) [11,12]. The solubility of CPEs in polar solvent is helpful in multilayer device fabrication and by using CPEs as ETLs, there is no need for matching cathode work function to the semiconductor lowest unoccupied molecular orbital (LUMO) energy level.

A number of CPEs have been reported with a diversity of backbone structures, charged groups and counterions [13,14]. Poly[9,9-bis[6′-(*N*,*N*,*N*-trimethylammonium)hexyl]fluorene-*alt*-*co*-1,4-phenylene] bearing different halide counteranions, PFPhX (X = F, Cl, Br, I, BIm_4), sodium poly[9,9-bis(4′-sulfonatobutyl)fluorene-*alt*-*co*-1,4-phenylene] $PFPhSO_3Na$, and sodium poly[9,9-bis(5′-pentanoate)fluorene-*alt*-*co*-1,4-phenylene] ($PFPhCO_2Na$) are some CPEs that have recently been investigated. The mechanism of the reduction in the electron injection barrier using the $PFPhBIm_4$ ETL thicker than 10 nm has proven to involve a rearrangement of the counterions within the ETL under the applied bias [15]. For thinner CPE ETLs, the reduced charge injection mechanism involves interfacial dipole formation between the ETL/cathode, modifying the work function of the cathode [16]. The effects of counterions on the efficiencies of solution-processed multilayer CPE-based PLEDs were examined by studying CPEs with the same poly[fluorene-co-phenylene] backbone [17]. The electronic [18], thermophysical [19], interfacial [20] properties and effect of thermal annealing [21] of these CPEs were also measured.

In view of the current interest in the CPEs, we set out to perform a theoretical study of the properties of some prototypical CPEs, in particular the working mechanism at the molecular level which is not well known yet. In this work, we consider the molecular structure and electronic properties of a series of typical CPEs including $PFPhCO_2Na$, $PFPhSO_3Na$, and $PFPhBIm_4$. The PFPh molecule is chosen as a reference for purpose of comparison. The structures of these molecules are presented in Figure 1. The three CPEs considered are divided into two groups in which group 1 includes CPEs with anionic pendant groups, $PFPhCO_2Na$ and $PFPhSO_3Na$, and group 2 CPE with cationic pendant groups, $PFPhBIm_4$. Some basic properties are investigated such as band gaps, energy levels, ionization energies (IEs), electron affinities (EAs), and charge transport properties. Comparison of the calculated properties between

* Corresponding author at: Department of Chemistry, University of Leuven, B-3001 Leuven, Belgium. Fax: +32 16 32 79 92.
E-mail address: minh.nguyen@chem.kuleuven.be (M.T. Nguyen).

0009-2614/$ - see front matter © 2012 Elsevier B.V. All rights reserved.
doi:10.1016/j.cplett.2012.01.080

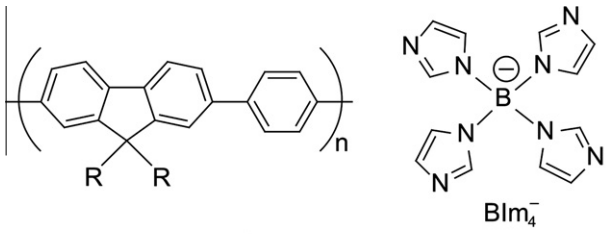

(a) R = C_6H_{13}
(b) R = $C_4H_8CO_2Na$
(c) R = $C_4H_8SO_3Na$
(d) R = $C_6H_{12}N(CH_3)_3BIm_4$

Figure 1. Chemical structures of (a) reference neutral conjugated polymer PFPh and three CPEs considered (b) $PFPhCO_2Na$, (c) $PFPhSO_3Na$, (d) $PFPhBIm_4$.

two groups with respect to the reference molecule, and between molecules in group 1, provides useful information about the effects of charged groups, counterions, and charge reversal on the properties of CPEs.

2. Computational details

All standard electronic structure calculations are performed using the GAUSSIAN 09 program [22]. Geometries of molecules PFPh with different side-chain lengths are first fully optimized using density functional theory (DFT) method with the hybrid B3LYP functional [23] and the split-valence 3-21G basis set, to examine the effect of side-chain length. In going from two to six $–CH_2–$ groups, the changes in HOMO–LUMO gaps are very small (0.000–0.002 eV). Based on these results, the side-chains of all monomers are truncated to two $–CH_2–$ groups in order to reduce the computational costs. Harmonic vibrational frequencies are also calculated at the B3LYP/3-21G level in order to establish the nature of the stationary points. Geometries of all neutral species considered are then re-optimized using a split-valence plus polarization basis set (B3LYP/SVP).

The band gap of each species is determined by calculating the electronic excitation energies using a time-dependent (TD) DFT method with the B3LYP functional. The IEs and EAs are calculated at the B3LYP/SVP and B3LYP/6–31+G(d)//B3LYP/SVP levels, respectively, as they are factors to be considered in the charge injection process. The values of IE and EA are obtained according to the adiabatic process, that is, from the difference in total energies between the ionized and ground states in their equilibrium geometries.

Internal reorganization energies of a hole and an electron are calculated according to the semi-classical Marcus theory [24] for each monomer using B3LYP/SVP energies. The electron coupling integral or transfer integral t_{12} was often calculated by the energy splitting in the 'dimer approach' in which the frozen orbital approximation is used to simplify the calculation. The electron coupling integral for the electron (hole) transport is approximated as half of the splitting of the LUMO–HOMO levels in a dimer made of two identical neutral molecules [25]. Coupling integrals were computed using the semi-empirical INDO (Intermediate Neglect of Differential Overlap) method [26] because it allows a treatment of very large systems. It has proven that the transfer integrals obtained from the INDO method are typically similar to or systematically 30% larger than DFT data. The latter are in the same order of magnitude as experimental values [26,27]. As the main purpose of the study is to compare the transfer integrals of different molecules, the limited accuracy of semi-empirical method is of little consequence on their relative values, as compared to the gain in computational cost. In this work the transfer integrals are calculated using the more recent semi-empirical PM6 method.

3. Results and discussion

3.1. Optimized geometries of the monomers

We first analyze the geometrical parameters of these monomers in both neutral and charged states. Comparison between the geometries of the charged and neutral states allows examining the effect on the backbone structures when adding or removing an electron from the neutrals. The torsional angles between fluorene and phenylene rings of monomers in neutral and charged states are listed in Table 1. An important feature of these materials is their capacity of maintaining to some extent the conjugation between adjacent aromatic groups at different torsional angles from their planes. All neutral monomers have relatively large torsional angles, ranging around 36–37°. The large torsional angles actually affect the π-overlap between rings and thus reduce linear π-conjugation of the monomers. The differences in torsional angles of the three CPEs, as compared with that of PFPh, are only of 0.3–0.9° and thus show that different counterions and charged groups have little effect on the torsional angles of neutral monomers. In group 1 the torsional angle of $PFPhCO_2Na$ is smaller than that of $PFPhSO_3Na$.

For monomers in cationic state, they all show a decrease in torsional angle as compared with the corresponding neutrals, and PFPh has the most near-planar structure. Removal of one electron has great effect on PFPh and group 1 CPEs with large decrease in torsional angles. The PFPh torsional angle in the cation amounts to 21°, being smaller than that of the neutral counterpart. For $PFPhCO_2Na$ and $PFPhSO_3Na$, the torsional angles decrease to 14° and 7°, respectively. However, for $PFPhBIm_4$ the effect is much smaller. The angle decreases only by 2°. These data shows that the conjugation tends to increase as one electron is removed from the molecules, but the degree of effect follows the ordering: PFPh > $PFPhCO_2Na$ > $PFPhSO_3Na$ ≫ $PFPhBIm_4$.

Addition of one electron to the monomers results in completely different results for the CPEs. Similar to the previous case, the torsional angle of PFPh anion remains the smallest. However, the torsion of $PFPhBIm_4$ becomes smaller than those of group 1 and now closer to that of PFPh anion. Two opposite effects of adding one electron can be noted. The PFPh planarity tends to increase greatly upon a sharp decreasing of torsional angle. However, for $PFPhCO_2Na$ and $PFPhSO_3Na$, the torsional angles turn out to increase slightly. For group 2, although the angle decrease of $PFPhBIm_4$ is not as large as that of PFPh, it is still large as compared to the small change in previous case.

Table 1 also lists the bond length variations following addition or removal of one electron. Clearly, electron removal induces greater effects on bond lengths of $PFPhCO_2Na$ and $PFPhSO_3Na$. On the other hand, electron injection mainly affects the bond lengths of $PFPhBIm_4$.

Besides the planarity, the A indices as defined by Julg [28] are also calculated by using the Eq. (1),

$$A = 1 - \frac{225}{n}\sum_{n}\left[\frac{(d_i - d_{avg})}{d_{avg}}\right]^2 \quad (1)$$

where n denotes the number of C–C bond, d_i and d_{avg} denote the individual and average bond length, respectively. A large value of A indicates a relatively small bond alternation and corresponds to a large delocalization. A scaling factor of 225 is used to force $A = 0$ for the Kekulé benzene (1,3,5-cyclohexatriene), a model chosen for alternating C–C bond lengths of 1.33 and 1.52 Å. For aromatic molecules such as benzene, all the bonds have the same length, being equal to the average bond length, leading thus to $A = 1$. The results are listed also in Table 1. In neutral and cationic states, the A indices of group 1 are nearly equal to that of PFPh and larger than that of group 2. The situation is reversed in anions where the A

Table 1
Torsional angles (°), inter-ring bond lengths (Å), average variations in bond length ($\Delta\bar{d}$, Å), and Julg indices A of four monomers (B3LYP/SVP).

Monomers	Torsional angle (°)			$\Delta\bar{d}$[a] (Å)		A (Julg indices)		
	Neutral	Cation	Anion	Cation	Anion	Neutral	Cation	Anion
PFPh	37.6	20.8	8.5	0.014	0.015	0.81	0.83	0.82
$PFPhCO_2Na$	36.7	23.3	36.8	0.014	0.000	0.81	0.84	0.81
$PFPhSO_3Na$	37.0	30.1	39.6	0.013	0.001	0.81	0.83	0.81
$PFPhBIm_4$	37.3	35.5	15.6	0.001	0.014	0.80	0.81	0.82

[a] Average variations in bond length (Å) are taken as average of absolute variations between the corresponding bond lengths of neutral and charged species.

index of $PFPhBIm_4$ is equal to that of PFPh (0.82) and marginally larger than those of group 1 (0.81). This theoretical calculation is supported by experimental results that electron mobilities for $PFPhBIm_4$, $PFPhCO_2Na$, and $PFPhSO_3Na$ are 8.3×10^{-7}, 1.1×10^{-8}, and 1.5×10^{-7} cm^2/Vs, respectively [29,30]. Larger counteranion (BIm_4^-) reduces the electron mobility by a factor of 14. This observation indicates that larger counteranion affects the molecular packing in the solid state. Altering the charge group (CO_2^- versus SO_3^-) has a large impact on the electron mobility.

3.2. Frontier orbitals and energy gaps

Similar to molecular orbital theory, the Kohn–Sham HOMO and LUMO energies obtained in density functional theory (DFT) are also connected with first ionization energy (IE) and electron affinity (EA), respectively. Since the exact exchange correlation functional is unknown, the assignment of a physical meaning to other Kohn–Sham orbitals is not clearcut. However, nearly linear correlation relationships have been found between higher HOMO energies and IEs, and between LUMO energies and lower EAs [31]. This supports the use of Kohn–Sham orbitals to semi-quantitatively estimate the molecular properties such as IEs, EAs, electronegativity, hardness, and excitation energies [32–34].

In general, introduction of charged groups and counterions results in a destabilization of HOMOs and stabilization of LUMOs of the monomers (Table 2). All other monomers have HOMO levels close to that of the reference. Electron injection is controlled by the height of the potential barrier at the interface, i.e., the difference between the LUMO level and the metal electrode's work function (Φ). As compared with $PFPhCO_2Na$ and $PFPhSO_3Na$, the LUMO level of $PFPhBIm_4$ is closer to the work functions of some commonly used metal electrodes, e.g. Sm ($\Phi = -2.7$ eV), Ba ($\Phi \approx -2.7$ eV), and Ca ($\Phi = -2.9$ eV).

Plots of frontier orbitals calculated at the B3LYP/SVP level are illustrated in Figure 2. The frontier orbitals of PFPh and other CPEs are very typical for conjugated polymers with HOMO having antibonding characteristics and LUMO having bonding characteristics, and both are delocalized over the entire backbone structure.

Poly[(9,9-bis(3'-((*N*,*N*-dimethyl)-*N*-ethylammonium)-propyl)-2,7-fluorene)-alt-1,4-phenylene] dibromide, has been synthesized and experimentally investigated [35]. The optical band gap of this molecule (2.92 eV) is very close to the optical band gap of 2.95–2.96 eV of the studied CPEs [18] (Table 2). The fact that band gap values for different monomers are similar due to the same conjugated backbone can be expected [13,14,18]. Therefore, we use the band gap of this molecule, which amounts to 3.6 eV, as a standard value for band gap of the CPEs with fluorenyl phenylene backbone.

Table 2
A comparison of frontier orbital energies (eV), HOMO–LUMO gaps (eV), lowest vertical excitation energies (eV) and experimental band gaps (eV).

Monomers	HOMO[a]	LUMO[a]	$\Delta E_{H\text{-}L}$[a]	Eg^{TDDFT}[b]	Eg^{Expt}[c]
PFPh	−5.78	−1.36	4.42	4.07	
$PFPhCO_2Na$	−5.31	−1.40	3.91	3.69	
$PFPhSO_3Na$	−5.67	−1.59	4.08	3.79	2.95
$PFPhBIm_4$	−5.28	−2.51	2.77	3.82	2.96

[a] HOMO, LUMO energies and HOMO–LUMO gaps were calculated at B3LYP/SVP level.
[b] Eg is determined from the lowest allowed electronic excitation energies calculated using a time-dependent TDDFT method at B3LYP/SVP level.
[c] Experimental optical band gaps are taken from Ref. [18].

The band gaps of PFPh and the CPEs presented in Table 2 are evaluated as the lowest allowed vertical excitation energies. The lowest allowed vertical excitation energies calculated at the B3LYP/SVP level of the three CPEs do not correspond to the LUMO ← HOMO transition ($PFPhSO_3Na$, $PFPhBIm_4$) or have only small contribution from this transition ($PFPhCO_2Na$). The calculated band gaps are in the range of 3.7–3.8 eV, and are quite close to the standard value of 3.6 eV.

3.3. Adiabatic ionization energies and electron affinities

The calculated adiabatic IEs and EAs of PFPh and the CPEs considered are summarized in Table 3. All monomers have the calculated EAs larger than that of PFPh but far smaller than the available experimental values [18]. The main reason for such a large deviation in electron affinity is the use of a rather small basis set in calculations. It is well known that much larger basis sets incorporating diffuse and polarization functions needs to be used for evaluating the EAs. Additionally, calculations are for single molecules in gas-phase whereas the experimental values were obtained from thin film.

As a low-lying LUMO level and high EA are desirable for efficient injection of electrons into a monomer, the $PFPhBIm_4$ having higher EAs is thus expected to be more efficient in electron addition.

All monomers have smaller vertical IE_v and adiabatic IE_a values than those of the reference PFPh. Decrease in IEs facilitates an injection of holes from metal electrodes into the HOMO of these materials. The calculated IEs are larger than the available experimental values for $PFPhSO_3Na$ and $PFPhBIm_4$. The average error between computational and experimental values is up 0.5 eV, which is large and also due to the basis set employed. Among the charged groups and counterions, the cationic charged group lower the IE more efficiently than the anionic charged groups.

3.4. Charge transport

The hole or electron transport can be described as a self-exchange reaction (1):

$$M^{\pm} + M \rightarrow M + M^{\pm}. \quad (1)$$

According to the semi-classical Marcus theory, the hopping rates for the self-exchange reactions are calculated from the Eq. (2):

$$k_{ET} = \frac{4\pi^2}{h}\frac{1}{\sqrt{4\pi\lambda k_B T}}t^2 \exp\left(-\frac{\lambda}{4k_B T}\right) \quad (2)$$

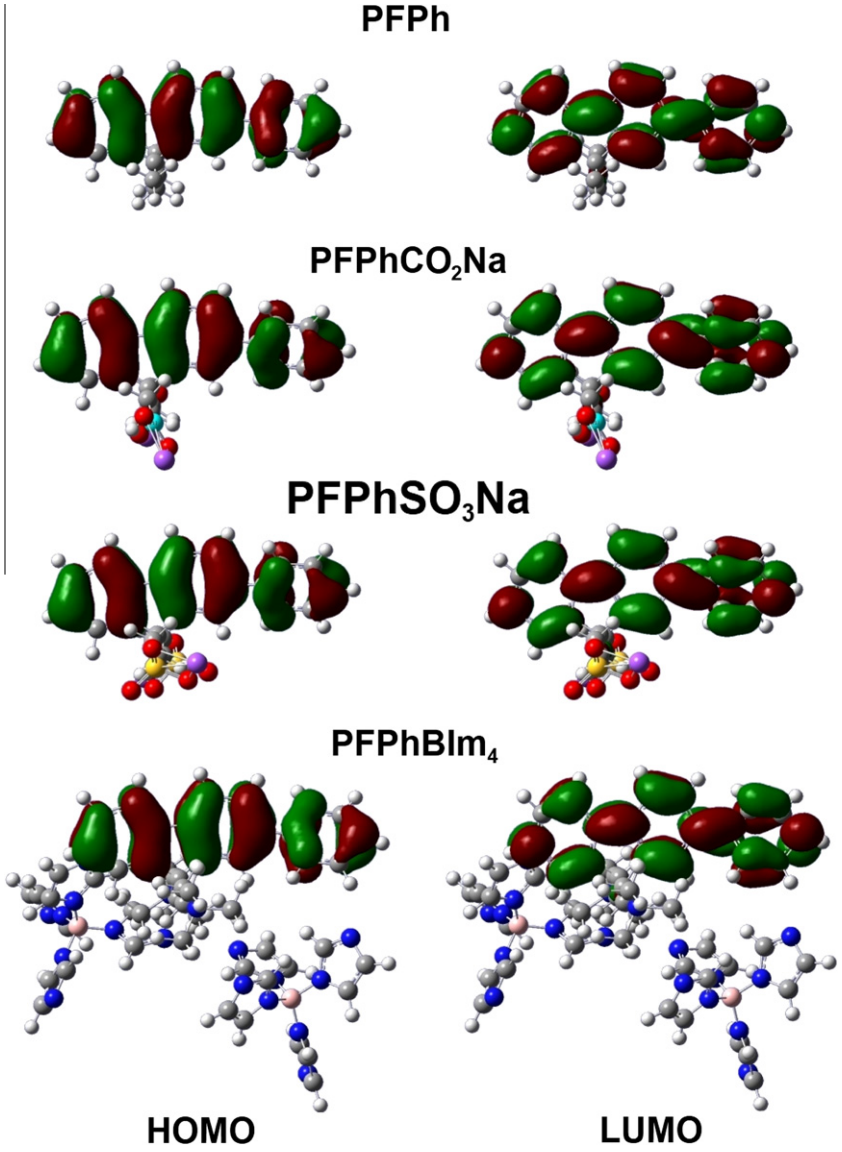

Figure 2. HOMO and LUMO of all monomers at the B3LYP/SVP level.

Table 3
Calculated (B3LYP/SVP) values for vertical, adiabatic ionization energies (IE_v, IE_a) and adiabatic electron affinities (EA_a). All values are in eV.

Monomer	IPs			EA_a	
	IE_v[a]	IE_a[a]	Expt[b]	EA_a[c]	Expt[b]
PFPh	7.17	7.02		0.45	
$PFPhCO_2Na$	6.64	6.47		0.90	
$PFPhSO_3Na$	7.03	6.60	6.15	1.03	3.20
$PFPhBIm_4$	6.54	6.19	6.17	1.88	3.21

[a] IE_v, IE_a were obtained from B3LYP/SVP calculations.
[b] Experimental data were taken from Ref. [18].
[c] EA_a were obtained from B3LYP/6-31+G*//B3LYP/SVP calculations.

These rates (and therefore the charge carrier mobilities) are determined by two major parameters:

(i) the first parameter is the electronic coupling, manifested by the transfer integral *t*, between adjacent molecules, which needs to be maximized, and
(ii) the second is the reorganization energy λ, which needs to be small for an efficient transport. The latter parameter contains an inner part and an outer part. The inner or intramolecular reorganization energy is a property of a single

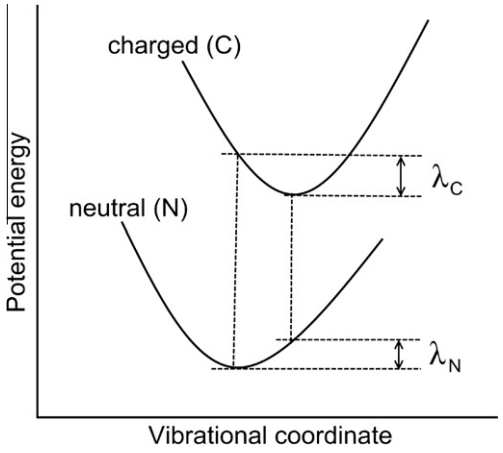

Figure 3. Descriptions of λ_C and λ_N through a schematic diagram of general adiabatic energy surfaces corresponding to ionization process.

Table 4
Relaxation energies $\lambda_C^{\pm}$, $\lambda_N^{\pm}$, reorganization energies $\lambda_{tot}^{\pm}$, transfer integrals (t_{12}, eV), and the hopping rates at room temperature $k_{298.15}$ (s^{-1}) of hole and electron transport processes (based on B3LYP/SVP data).

Monomer	Hole transport					Electron transport				
	λ_C^+	λ_N^+	λ_{tot}^+	t_{12}^+	$k_{298.15}^+$	λ_C^-	λ_N^-	λ_{tot}^-	t_{12}^-	$k_{298.15}^-$
PFPh	0.15	0.14	0.29	0.267	1.33E+14	0.35	0.06	0.41	0.089	3.83E+12
PFPhCO2Na	0.16	0.11	0.27	0.289	1.96E+14	0.07	0.02	0.09	0.073	1.23E+14
PFPhSO3Na	0.42	0.43	0.85	0.315	4.62E+11	0.08	0.07	0.15	0.093	8.68E+13
PFPhBIm4	0.28	0.29	0.57	0.004	1.45E+09	0.33	0.52	0.85	0.052	1.28E+10

molecule and consists of two relaxation energies, λ_C and λ_N, going from neutral to charged states and the reverse, as illustrated in Figure 3. The outer reorganization energy deals with the medium polarization and is typically on the order of tenth(s) of an electron-volt. It follows that the inner reorganization energy and transfer integral are the magnitudes to be controlled when seeking for an efficient charge injection and high electron-transfer rate [36].

3.4.1. Reorganization energies

There are two ways of computing reorganization energies. The first is a method based on adiabatic processes whereas the second method is based on normal-mode analysis [37]. In this work, we calculate the reorganization energy using the first method with the adiabatic potential energy surface as shown in Figure 2. The total adiabatic reorganization energy, as expressed in Eq. (3), is a sum of two relaxation energies given in Eqs. (4) and (5):

$$\lambda_{tot}^{\pm} = \lambda_C^{\pm} + \lambda_N^{\pm} \quad (3)$$

$$\lambda_C^{\pm} = E_C^{rel} - E_C \quad (4)$$

$$\lambda_N^{\pm} = E_N^{rel} - E_N \quad (5)$$

where E_C^{rel} is the energy of the charged state in the optimized geometry of the neutral molecule, E_N^{rel} is the energy of the neutral state in the optimized geometry of the charged molecule, superscript + and – denote the hole-transport process and electron-transport process, respectively. The reliability of DFT methods has been shown in reasonably reproducing the charge transport properties [27]. We thus use the B3LYP/SVP level with unrestricted DFT formalism to optimize geometries of molecules in both cationic and anionic states.

The calculated relaxation energies $\lambda_C^{\pm}$, $\lambda_N^{\pm}$ and reorganization energies $\lambda_{tot}^{\pm}$ are summarized in Table 4. Different from the hole transport process in which the λ_C^+ and λ_N^+ values are approximately equal, in the electron transport process, these two components are in some cases very different from each other. The values of λ_{tot}^+ and λ_{tot}^- are within the range 0.3–0.8 eV and 0.1–0.9 eV, respectively. Except for $PFPhCO_2Na$, the λ_{tot}^+ values turn out to be increased as compared with that of PFPh. In the electron transport process, the reorganization energies of group 1 decrease by small values (0.1 and 0.2 eV), these values are smaller than those reported for organic n-type materials such as fluoarene–oligothiophenes (0.2–0.3 eV), and pentacene (0.13 eV). $PFPhBIm_4$ has larger reorganization energy for electron transport process than the group 1 monomers which could lead to lower electron-transfer rate.

3.4.2. Transfer integrals

Since the monomers considered have rather large side chain groups which prevent two chains to be close to each other in a *syn* disposition, we construct a dimer of two neutral molecules, wherein two chains are disposed in an *anti*-configuration (cf. Figure 4). The intermolecular distance is chosen to be 3.0 Å. Since

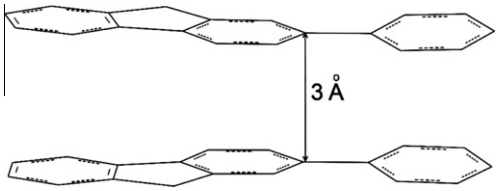

Figure 4. Schematic shape of two superimposed monomers. The side chain groups and hydrogen atoms are omitted for a better view of backbone structure.

all the monomers have large dihedral angles between the two rings and therefore, it is difficult to build a parallel structure with adequate intermolecular distance. Here it is taken as the distance between the bonds connecting both fluorene and phenylene rings. The dimeric structures are built in such a way that when looking from the direction vertical to the fluorene ring, the two connecting bonds are superimposed on each other. The dihedral angle formed between two bonds varies from −15° to 15° in order to recover the best position between both molecules. The calculated results point out that the dihedral angle of 0° yields the largest transfer integrals for most of the studied CPEs (cf. Supporting information). The transfer integrals in hole- and electron-transport processes $t_{12}^{\pm}$ of the CPEs obtained from the dimeric structures with the dihedral angle 0° are given in Table 4.

The t_{12}^+ values of the anionic CPEs are larger than that of PFPh and much larger than that of the cationic CPE, $PFPhBIm_4$. The t_{12}^- values of the CPEs vary differently as compared to that of the reference PFPh. For $PFPhCO_2Na$ and $PFPhBIm_4$, the values of t_{12}^- are smaller while t_{12}^- of $PFPhSO_3Na$ is larger. $PFPhBIm_4$ has the largest t_{12}^- value among the CPEs examined, which appear to facilitate the electron transport. This observation agrees well with the experimental result that $PFPhBIm_4$ has the highest electron mobility among the CPEs studied here. Comparison between t_{12}^+ and t_{12}^- shows that group 1 have larger t_{12}^+ than t_{12}^- while a reverse trend holds for group 2. In the latter, the electron transfer integral is much larger than the hole counterpart.

Since the dependence of hopping rate on transfer integrals and/or on reorganization energies is not linear, a comparison of these parameters alone cannot be used to make a conclusion about the transfer rates. Therefore, calculations of the hopping rates of the CPEs at room temperature are carried out and also listed in Table 4. However, due to the lack of the experimental data of the intermolecular distances between the rings, the absolute values of the transfer integrals and thus the hopping rates should be considered with much caution. Instead, we would concentrate on a comparison of the relative hopping rates in hole- and electron-transport processes in an attempt to determine whether the CPEs are better in hole or electron transport. From the computed results, $PFPhCO_2Na$ appears to be hole and electron transport at nearly equal rates. Meanwhile, different from PFPh, the other two CPEs ($PFPhSO_3Na$ and $PFPhBIm_4$) seem to favor electron-transport over hole-transport.

4. Concluding remarks

We investigate the molecular structures and electronic properties of a series of CPE monomers with the same backbone but different pendant groups. A geometrical analysis shows that the monomers have relatively large torsions in their neutral states. When adding or removing one electron, the torsional angles tend to decrease. In case of hole injection, the bond lengths of $PFPhCO_2$-Na and $PFPhSO_3Na$ vary greatly. Meanwhile, an electron injection induces a larger effect on $PFPhBIm_4$.

Calculated results of frontier orbitals and band gaps are also presented. The charged groups and counterions turn out to cause little effects on the band gaps, which agree well with the experimental results. The theoretical band gaps calculated using TDDFT are in good agreement with the standard band gap for this type of CPEs. Reorganization energy and transfer integral data along with geometrical analysis suggest that the molecules $PFPhSO_3Na$ and $PFPhBIm_4$ constitute good materials for ETLs since the corresponding rates of transporting electron of these CPEs are larger. We hope that these theoretical results are helpful in assisting experiments designed for a better performance of the electronic properties of the CPEs, improving the optimal structures and thereby increasing the performance of PLEDs.

Acknowledgments

The authors are indebted to the KULeuven Research Council (GOA, IDO and IUAP programs) and the European Erasmus Mundus Master in Theoretical Chemistry and Computational Modeling (TCCM) for support.

Appendix A. Supplementary data

Supplementary data associated with this article can be found, in the online version, at doi:10.1016/j.cplett.2012.01.080.

References

[1] M.R. Pinto, K.S. Schanze, Synthesis (2002) 1293.
[2] A.O. Patil, Y. Ikenoue, F. Wudl, A.J. Heeger, J. Am. Chem. Soc. 109 (1987) 1858.
[3] T.I. Wallow, B.M. Novak, J. Am. Chem. Soc. 113 (1991) 7411.
[4] T.A. Skotheim, J.R. Reynolds, Conjugated Polymers: Theory, Synthesis, Properties, and Characterization, CRC Press, Boca Raton, FL, 2007.
[5] C. Holm, M. Rehahn, W. Oppermann, M. Ballauf, Adv. Polym. Sci. 166 (2004) 1.
[6] S.K. Tripathy, J. Kumar, H.S. Nalwa, Handbook of Polyelectrolytes and Their Applications, American Scientific Publishers, Stevenson Ranch, CA, 2002.
[7] C. Chi, A. Mikhailovsky, G.C. Bazan, J. Am. Chem. Soc. 129 (2007) 11134.
[8] S.W. Thomas, G.D. Joly, T.M. Swager, Chem. Rev. 107 (2007) 1339.
[9] Z. Gu, Q.-D. Shen, J. Zhang, C.-Z. Yang, Y.-J. Bao, J. Appl. Polym. Sci. 100 (2006) 2930.
[10] L. Edman, B. Liu, M. Vehse, J. Swensen, G.C. Bazan, A.J. Heeger, J. Appl. Phys. 98 (2005) 44502.
[11] S.-H. Oh, S.-I. Na, Y.-C. Nah, D. Vak, S.-S. Kim, D.-Y. Kim, Org. Electron. 8 (2007) 773.
[12] M.B. Ramey, J. Hiller, M.F. Rubner, C. Tan, K.S. Schanze, J.R. Reynolds, Macromolecules 38 (2005) 234.
[13] C.V. Hoven, A. Garcia, G.C. Bazan, T.Q. Nguyen, Adv. Mater. 20 (2008) 3793.
[14] R. Yang, A. Garcia, D. Korystov, A. Mikhailovsky, G.C. Bazan, T.Q. Nguyen, J. Am. Chem. Soc. 128 (2006) 16532.
[15] C. Hoven, R. Yang, A. Garcia, A.J. Heeger, T.Q. Nguyen, G.C. Bazan, J. Am. Chem. Soc. 129 (2007) 10976.
[16] H.B. Wu, F. Huang, Y.Q. Mo, W. Yang, D.L. Wang, J.B. Peng, Y. Cao, Adv. Mater. 16 (2004) 708.
[17] A. Garcia, J.Z. Brzezinski, T.Q. Nguyen, J. Phys. Chem. C 113 (2009) 2950.
[18] J.H. Seo, T.Q. Nguyen, J. Am. Chem. Soc. 130 (2008) 10042.
[19] J.H. Ortony, R. Yang, J.Z. Brzezinski, L. Edman, T.Q. Nguyen, G.C. Bazan, Adv. Mater. 20 (2008) 298.
[20] C. Wang et al., J. Am. Chem. Soc. 131 (2009) 12538.
[21] C.-Y. Lin, A. Garcia, P. Zalar, J.Z. Brzezinski, T.Q. Nguyen, J. Phys. Chem. C 114 (2010) 15786.
[22] Gaussian 09, Revision A.02, Gaussian, Inc.: Wallingford CT, 2009.
[23] R. Parr, W. Yang, Density Functional Theory of Atoms and Molecules, Oxford University Press, New York, 1989.
[24] R.A. Marcus, Rev. Mod. Phys. 65 (1993) 599.
[25] V. Coropceanu, J. Cornil, D.A. da Silva Filho, Y. Olivier, R. Silbey, J.-L. Brédas, Chem. Rev. 107 (2007) 926.
[26] V. Lemaur et al., J. Am. Chem. Soc. 126 (2004) 3271.
[27] J.L. Brédas, D. Beljonne, V. Coropceanu, J. Cornil, Chem. Rev. 104 (2004) 4971.
[28] A. Julg, P. François, Theoret. Chim. Acta (Berl.) 7 (1967) 249.
[29] A. Garcia, J.Z. Brzezinski, Y. Jin, B. Walker, T.Q. Nguyen, Appl. Phys. Lett. 91 (2007) 153502.
[30] A. Garcia, Y. Jin, J.Z. Brzezinski, T.-Q. Nguyen, J. Phys. Chem. C 114 (2010) 22309.
[31] J. Zhan, J. Phys. Chem. A 107 (2003) 4184.
[32] N.N. Pham-Tran, M.T. Nguyen, Comp. Rend. Acad. Sci. (C.R. Chimie) 13 (2010) 912.
[33] D. Delaere, M.T. Nguyen, L.G. Vanquickenborne, Phys. Chem. Chem. Phys. 4 (2002) 1522.
[34] D. Delaere, M.T. Nguyen, L.G. Vanquickenborne, J. Organometal, Chemistry 643–644 (2002) 194.
[35] F. Huang, H. Wu, D. Wang, W. Yang, Y. Cao, Chem. Mater. 16 (2004) 708.
[36] G. García, A. Garzón, J.M. Granadino-Roldán, M. Moral, A. Navarro, M. Fernández- Gómez, J. Phys. Chem. C 115 (2011) 6922.
[37] Y.H. Park, Y.-H. Kim, S.K. Kwon, I.S. Koo, K. Yang, Bull. Korean Chem. Soc. 31 (2010) 1649.